JOURNAL OF MODERN OPTICS, 20 JANUARY–15 FEBRUARY 2005
VOL. 52, NO. 2–3, 201–219

Taylor & Francis
Taylor & Francis Group

Phase stabilization of mode-locked lasers

STEVEN T. CUNDIFF and JUN YE
JILA, National Institute of Standards and Technology and University of Colorado, Boulder, Colorado, 80309-0440, USA;
e-mails: cundiffs@jila.colorado.edu; ye@jila.colorado.edu
tel: +1(303)492-7848; fax: +1(303)735-0101

(*Received 23 July 2004*)

Abstract. We present results on carrier-envelope phase stabilization of mode-locked lasers. The carrier-envelope phase of femtosecond optical pulses becomes important when they are used to probe attosecond physics. We demonstrate that long-term carrier-envelope phase stability is possible to achieve. Using phase-stable lasers it is possible to combine the output of different lasers phase coherently. It is also possible to load them phase coherently into a cavity, yielding the prospect of high-intensity experiments without an amplifier. Finally, we present quantum interference control of injected currents in semiconductors, which provides a solid-state phase detector of the carrier-envelope phase.

All current techniques for accessing attosecond time scales rely on processes that are sensitive to the electric field of femtosecond pulses. Control of the electric field at an attosecond level requires control of the phase of the femtosecond pulse, specifically the phase of the carrier wave with respect to the envelope, which is known as the carrier-envelope phase ϕ_{CE}. For example, changing ϕ_{CE} by 0.1 rad shifts the electric field by 45 as for an 800 nm pulse. This clearly implies that techniques to stabilize ϕ_{CE} have an impact on attosecond science.

The application of techniques for precision stabilization of single-frequency continuous-wave (CW) lasers to mode-locked lasers has enabled control of the evolution of the carrier envelope phase of the intracavity pulse. The evolution of the carrier-envelope phase is manifest as an overall frequency shift in the output spectrum of the lasers. By using a self-referencing technique, this frequency shift can be measured and used in a feedback loop to stabilize the phase evolution. Furthermore, similar concepts and techniques can be used to cross-lock two mode-locked lasers coherently, thereby 'stitching' their output spectra together.

In this paper, we first introduce the basic concepts of carrier-envelope phase evolution in mode-locked lasers. Using these concepts, we then present results on stabilization of ϕ_{CE} and on locking two femtosecond lasers to obtain a single coherent output. Building on the same concepts, we demonstrate results on coherent addition of femtosecond pulses using a passive optical cavity for pulse

Journal of Modern Optics ISSN 0950–0340 print/ISSN 1362–3044 online
http://www.tandf.co.uk/journals
DOI: 10.1080/09500340412331303252

amplification. These discussions are followed by the demonstration of quantum interference control of injected photocurrents in semiconductors, which can be used to detect ϕ_{CE}. We finish by briefly mentioning the impact that these techniques are having on the field of optical frequency metrology and optical atomic clocks.

The concept of the carrier-envelope phase is based on the decomposition of the pulses into an envelope function $\hat{E}(t)$ that is superimposed on a continuous carrier wave with frequency ω_c, so that the electric field of the pulse is written $E(t) = \hat{E}(t)e^{i\omega_c t}$. The carrier-envelope phase ϕ_{CE} is the phase shift between the peak of the envelope and the closest peak of the carrier wave. In any dispersive material, the difference between group and phase velocities will cause ϕ_{CE} to evolve as the pulse propagates.

Mode-locked lasers generate short optical pulses by establishing a fixed-phase relationship between all of the lasing longitudinal modes. (For a textbook level discussion, see [1].) Mode locking requires a mechanism that results in a higher net gain for short pulses compared with CW operation. This mechanism can be either an active element or implemented passively with saturable absorption (real or effective). Passive mode locking yields the shortest pulses because, up to a limit, the self-adjusting mechanism becomes more effective as the pulse shortens [2]. Real saturable absorption occurs in a material with a finite number of absorbers, for example a dye or semiconductor. The shortness of the pulses is limited by the finite lifetime of the excited state. Effective saturable absorption typically uses the nonlinear index of refraction of some material together with spatial effects, polarization or interference to produce higher net gain for shorter pulses. The ultimate limit on minimum pulse duration in such a mode-locked laser is due to the interplay between the mode-locking mechanism, group velocity dispersion (GVD) and net gain bandwidth [2].

Currently, the generation of ultrashort optical pulses is dominated by the Kerr-lens mode-locked Ti : sapphire laser because of its robust performance, ultrawide bandwidth and relative simplicity. Kerr-lens mode locking (KLM) is based on a combination of self-focusing in the Ti : sapphire crystal and an aperture that selects the spatial mode corresponding to the presence of self-focusing. The Ti : sapphire crystal is pumped by green light from either an Ar^+-ion laser or a diode-pumped solid-state laser, which provides far superior performance in terms of laser stability and noise. The Ti : sapphire crystal provides gain and serves as the nonlinear material for mode locking. Prisms or dispersion-compensating mirrors compensate the GVD in the gain crystal [3]. Since the discovery of KLM [4, 5], the pulse width obtained directly from mode-locked lasers has been shortened by approximately an order of magnitude by first optimizing the intracavity dispersion [6] and then using dispersion-compensating mirrors [7, 8] to create pulses that are less than 6 fs in duration, that is less than two optical cycles. Recently, output spectra that span an octave (factor of two in optical frequency) have been obtained directly from a mode-locked laser [9, 10], which is an important accomplishment for phase stabilization.

To understand how frequency-domain techniques can be used to control mode-locked lasers, we must first connect the time- and frequency-domain descriptions [11, 12]. To start, we ignore the carrier-envelope phase and assume identical pulses; that is, ϕ_{CE} is a constant. If we just consider a single pulse, it will have a power spectrum that is the Fourier transform of its envelope function and is

centred at the optical frequency of its carrier. Generally, for any pulse shape, the frequency width of the spectrum will be inversely proportional to the temporal width of the envelope. For a train of identical pulses, separated by a fixed interval, the spectrum can easily be obtained by a Fourier series expansion, yielding a comb of regularly spaced frequencies, where the comb spacing is inversely proportional to the time between pulses; that is, it is the repetition rate f_{rep} of the laser that is producing the pulses. The Fourier relationship between time and frequency resolution guarantees that any spectrometer with sufficient spectral resolution to distinguish the individual comb lines cannot have enough temporal resolution to separate successive pulses. Therefore, the successive pulses interfere with each other inside the spectrometer and the comb spectrum occurs because there are certain discrete frequencies at which the interference is constructive. Using the result from Fourier analysis that a shift in time corresponds to a linear phase change with frequency, we can readily see that the constructive interference occurs at frequencies nf_{rep}, where n is an integer.

When ϕ_{CE} is evolving with time, such that from pulse to pulse (at a time separation of $T = 1/f_{\mathrm{rep}}$) there is a phase increment of $\Delta\phi_{\mathrm{CE}}$, then in the spectral domain a rigid shift will occur for the frequencies at which the pulses add constructively. This shift is easily determined to be $(1/2\pi)\,\Delta\phi_{\mathrm{CE}}/T$. Thus the optical frequencies ν_n of the comb lines are $\nu_{\mathrm{n}} = nf_{\mathrm{rep}} + f_0$, where n is a large integer of the order of 10^6 that indexes the comb line and f_0 is the comb offset due to the pulse-to-pulse phase shift. The comb offset is connected to the pulse-to-pulse phase shift by $f_0 = (1/2\pi)f_{\mathrm{rep}}\,\Delta\phi_{\mathrm{CE}}$. The relationship between time- and frequency-domain pictures is summarized in figure 1. The pulse-to-pulse change in the phase for the train of pulses emitted by a mode-locked laser occurs because the phase and group velocities inside the cavity are different. Thus, $\Delta\phi_{\mathrm{CE}}$ can be expressed in terms of the average phase velocity v_{p} and group velocity v_{g} inside the cavity. Specifically, $\Delta\phi_{\mathrm{CE}} = (1/v_{\mathrm{g}} - 1/v_{\mathrm{p}})l_c\omega_c$, where l_{c} is the round-trip length of the laser cavity and ω_{c} is the 'carrier' frequency.

From this discussion, we see that stabilizing the evolution of the carrier-envelope phase, that is fixing the value of $\Delta\phi_{\mathrm{CE}}$, is equivalent to fixing the value of f_0. Although it is possible to measure $\Delta\phi_{\mathrm{CE}}$ directly by comparing successive pulses [13, 14], measurement of f_0 in the frequency domain is much more sensitive as it effectively samples pulses with much greater temporal separations.

The most common method for measuring f_0 is self-referencing [14–16], which is shown schematically in figure 2. In self-referencing, the low-frequency wing of the spectrum is frequency doubled and compared with the high-frequency wing by heterodyning them against one another. The heterodyne beat provides the difference frequency, which by simple arithmetic is just f_0. The key challenge to self-referencing is obtaining sufficient spectral breadth so that spectral overlap occurs between the doubled low frequencies and the original high frequencies; this overlap obviously requires that the original frequencies are a factor of two apart (i.e. the spectrum spans an octave). An octave span can be achieved by spectral broadening external to the laser, typically in a microstructure optical fibre [17, 18]. However, octave-spanning spectra have also been obtained directly from mode-locked Ti : sapphire lasers [9, 10]. It is also possible to use an auxiliary CW laser [19–21]; however, this technique is more commonly used in optical frequency metrology experiments.

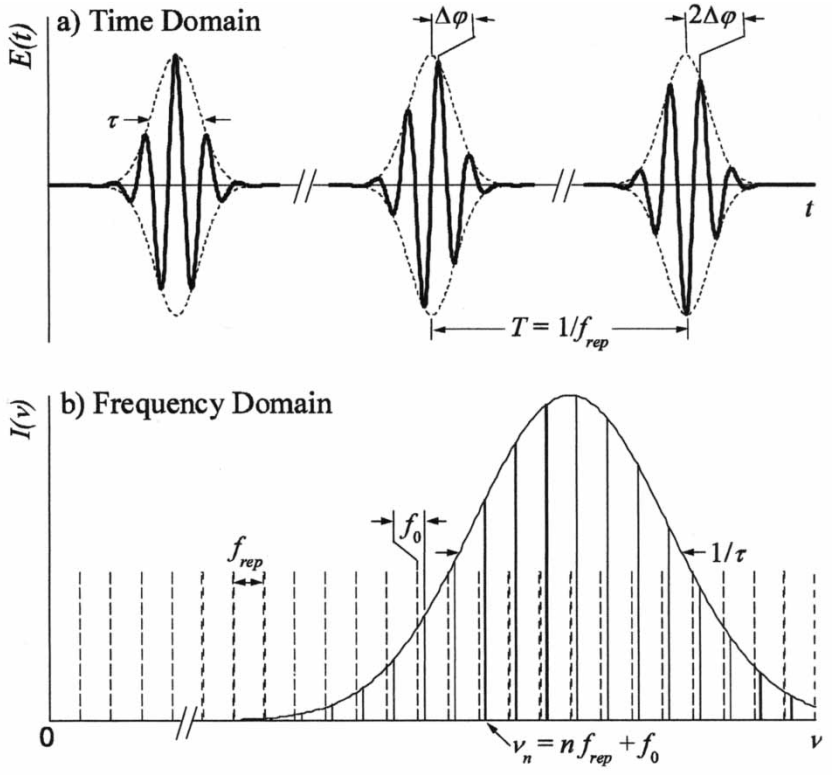

Figure 1. Summary of the time–frequency correspondence for a pulse train with evolving carrier-envelope phase.

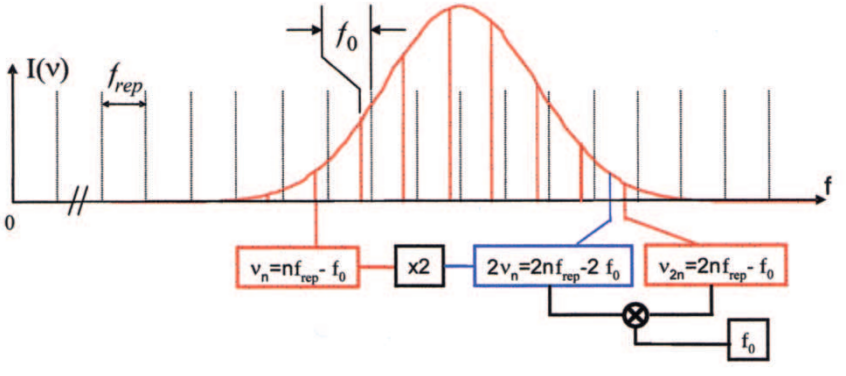

Figure 2. Schematic diagram of the self-referencing technique used to determine the offset frequency f_0 of the spectral comb.

Measurement of the carrier-envelope phase coherence characterizes how well the stabilization is working. This is done by closely examining the frequency- and phase-noise power spectral densities (PSDs) of f_0. Physically, the carrier-envelope phase coherence simply reflects how well we can tell what the carrier-envelope phase is of a given pulse in the train if we know the phase of an earlier pulse.

Knowing the carrier-envelope phase of a given pulse is important, however, for coherent pulse synthesis because we need to maintain carrier-envelope coherence between the two lasers. For experiments sensitive to ϕ_{CE}, it is important that ϕ_{CE} is well determined during the measurement process in order to reveal how ϕ_{CE} affects the outcome.

The evolution of the carrier-envelope phase is directly related to the laser offset frequency via $\phi_{CE} = 2\pi f_0 t + \phi_0$. If f_0 is stabilized to a frequency derived from the laser repetition rate, the value of f_0 fixes the pulse-to-pulse phase shift in the carrier-envelope phase, $\Delta\phi_{CE} = 2\pi f_0/f_{rep}$. The constant offset ϕ_0, often termed the 'absolute phase', determines the initial phase shift (at $t = 0$) between the carrier and the pulse envelope, making it an important parameter in field-sensitive experiments [22, 23]. The residual fluctuations of f_0 around its mean value, as manifested in the frequency- or phase-noise PSD around the carrier, allow determination of the stability of ϕ_{CE}, which in turn determines the duration of a phase-sensitive measurement for ultrafast experiments. To address the feasibility of phase-sensitive experiments, we present coherence time measurements of a stabilized Ti : sapphire laser. These measurements, aside from determining the time scale over which the light pulses remain coherent, also give the quality of the servo system and aid in identifying various noise contributing sources within the stabilization loop.

Knowledge of the stability of the offset frequency directly yields that of the carrier-envelope phase. The stability of the offset frequency is determined from its frequency-domain lineshape. The noise analysis is straightforward since the spectrum of noise side bands at frequency offsets f relative to the carrier yield the PSD, $S(f)$, of the phase noise [24]:

$$\Delta\phi_{rms}|_{\tau_{obs}} = \left(2\int_{1/(2\pi\tau_{obs})}^{\infty} S(f)\mathrm{d}f\right)^{1/2}. \quad (1)$$

Integration of the noise spectrum yields the total accumulated phase error $\Delta\phi_{rms}$ on ϕ_{CE}. Specifically, integration of $S(\nu)$ up to an observation time τ_{obs} over which $\Delta\phi_{rms}$ accumulates about 1 rad is generally taken to define the coherence time τ_{coh}.

We determine the carrier-envelope phase coherence time of a stabilized Kerr-lens mode-locked Ti : sapphire laser capable of producing 10 fs pulses. The laser uses prisms for intracavity dispersion compensation [3]. The laser baseplate is temperature controlled and the laser itself is encased in a pressure-sealed box. Negative feedback is obtained with a bandwidth of about 18 kHz via tilting the laser end mirror using a piezoelectric actuator. To perform an out-of-loop measurement of the offset frequency phase noise, we utilize two ν-to-2ν interferometers to implement the self-referencing scheme shown in figure 2 [25]. One interferometer stabilizes the laser, while the second determines the carrier-envelope phase noise from a phase-sensitive measurement of f_0. The phase noise PSD is obtained by mixing f_0 down to the base band where the noise side bands are measured using a fast-Fourier transform spectrum analyser (figure 3).

Figure 4 presents the results of the coherence measurement. Measurement of both the unstabilized offset frequency and the frequency f_0 used for locking are included; comparison of the two indicates the noise suppression by the stabilization loop. The latter provides an in-loop phase noise measurement that is used only to determine the effectiveness of the stabilization circuitry. The difference

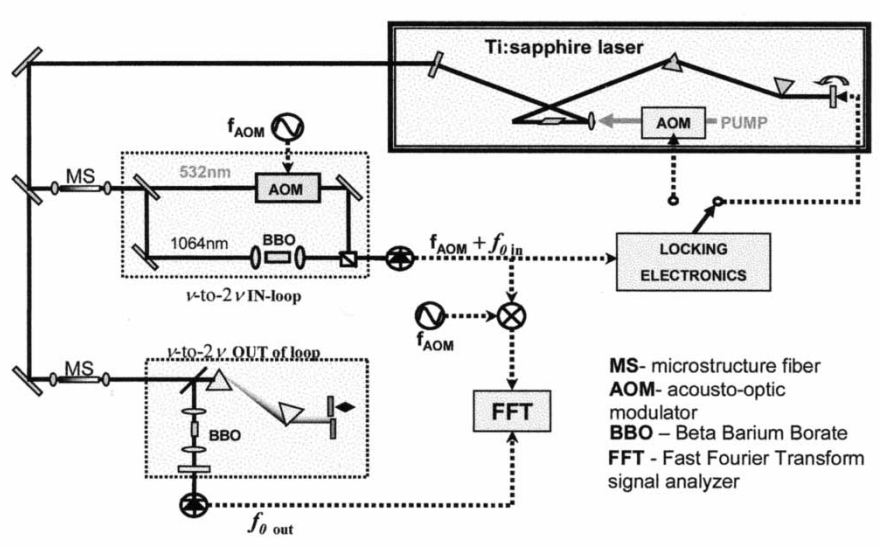

Figure 3. Experimental set-up showing how the coherence of ϕ_{CE} is measured. One interferometer is used to stabilize the laser while the second ν-to-2ν interferometer determines the phase coherence. The noise of the second interferometer is minimized by making the ν-to-2ν comparison as common mode as possible by using prisms for spectral dispersion.

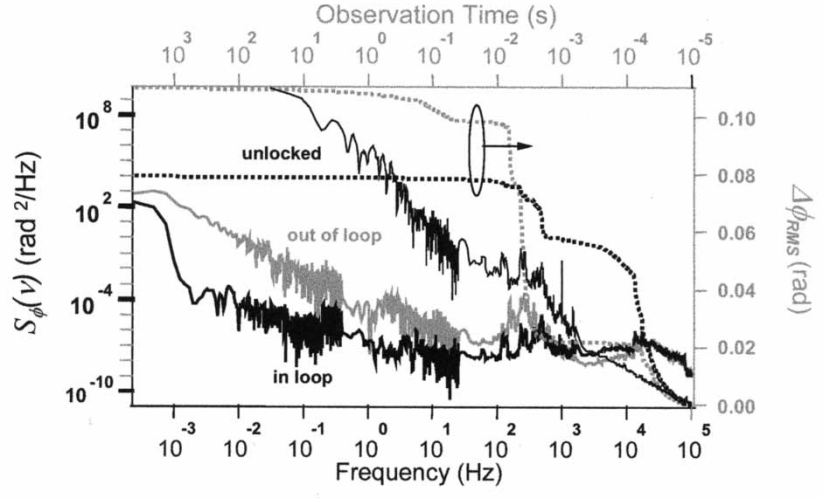

Figure 4. Phase PSD $S(\nu)$ (left axis) for the in-loop (—) and out-of-loop spectra (- - -) of the comb offset frequency (bottom axis). Integration of $S(\nu)$ yields the accumulated phase error (right axis) as a function of observation time (top axis).

between the out-of-loop and in-loop spectra yields the extracavity phase noise present within the stabilization loop (e.g. from the feedback electronics, the ν-to-2ν interferometer, the microstructure fibre, etc.) and the differential noise between the two loops. This noise is written on to the output of the laser, as the servo

system uses the laser to compensate for extracavity noise. Integration of the phase noise PSD out of loop (in loop) in figure 4 results in an accumulated phase error of 0.109 rad (0.08 rad) over the interval 102 kHz down to 488 mHz (which is resolution limited). Given that the out-of-loop accumulated phase error is less than 1 rad, the lower frequency integration bound determines a lower limit of the coherence time $\tau_{coh} = 1/(2\pi \times 244\,\mu\text{Hz}) = 652\,\text{s}$. This indicates that phase coherence is maintained for more than 65×10^9 pulses.

We would like to emphasize that carrier-envelope phase coherence is not the same as optical coherence. A process that shifts the temporal position of the pulse without changing the ϕ_{CE} of the pulse destroys the optical coherence but does not affect the carrier-envelope phase coherence.

Aside from the problems posed by fibre-induced phase fluctuations, stabilization of Ti : sapphire laser using microstructure fibre presents challenges to short-pulse experiments due to fibre dispersion. Additionally, complexities in the fibre alignment often lead to loss of fibre coupling and degradation in the f_0 signal over time. This degradation hinders optical frequency metrology since long-term averaging is necessary to increase the measurement precision. Thus, a laser that directly generates an octave is preferable. We present an octave-spanning conventional-geometry Ti : sapphire laser using intracavity prisms and negatively chirped mirrors. This has the advantage over a previously demonstrated octave-spanning laser [9, 26] in that the laser does not require precise intracavity dispersion compensation, nor does it require the use of an auxiliary space and time focus. We support the definition of octave spanning by demonstrating stabilization of the carrier-envelope phase using the bandwidth from the laser alone.

The octave-spanning laser presented here is an x-folded cavity that utilizes CaF_2 prisms and commercially available negative-chirped mirrors for intracavity dispersion compensation (figure 5). The generation of intracavity continuum is obtained via optimization of self-phase modulation in the laser crystal. The latter is obtained by strong misalignment of the curved mirrors away from the optimal CW position, which results in the production of a highly asymmetric and highly focused CW beam. When pumped with 5.5 W of 532 nm light, the mode-locked

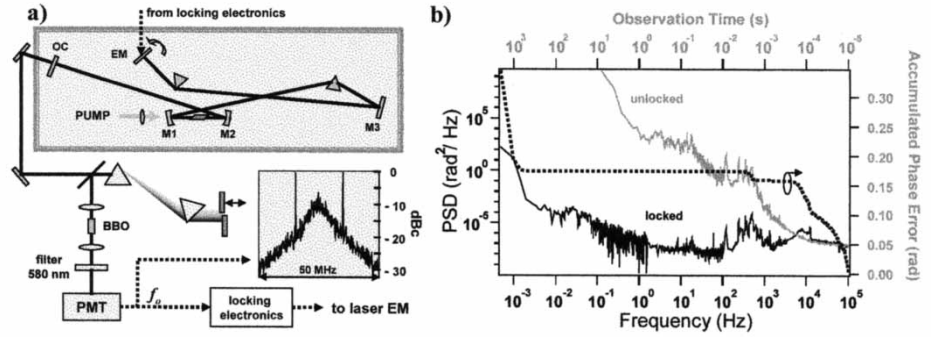

Figure 5. (a) Experimental schematic diagram of the octave-spanning Ti : sapphire laser and the ν-to-2ν interferometer used for measurement of the laser offset frequency. The inset shows the rf spectrum of f_0 at a 100 kHz resolution bandwidth. (b) Phase-noise PSD (left axis) of the stabilized f_0 versus frequency (bottom axis) and the integrated phase error (right axis) as a function of observation time (top axis).

laser spectrum spans from 580 to 1200 nm (about 40 dB down from the 800 nm portion of the spectrum) with an average power of 400 mW (100 mW CW) at an approximately 100 MHz repetition rate [10].

To demonstrate that the spectrum is indeed octave spanning, we measure f_0 using the laser output directly, that is without external broadening. This is done with a ν-to-2ν interferometer that uses prisms for spectral dispersion (not for compression) as shown in figure 5. The beat signal is detected using a fast photomultiplier tube and yields a maximum signal-to-noise ratio of about 30 dB at 100 kHz resolution bandwidth. This signal is then used to stabilize the laser using the piezoelectric actuator scheme described earlier. Figure 5 (b) presents the stabilization results. The phase noise PSD presented is an in-loop measurement of the offset frequency, which, as explained previously, may not reflect the total noise on the laser output. However, the use of the octave spanning laser eliminates microstructure fibre noise. Interferometer noise is also minimized by making the ν-to-2ν comparison as common mode as possible. As a result, the main contribution to the out-of-loop phase noise should be less than that shown in figure 4.

An interesting aspect of the generated continuum is the laser beam spatial profile as a function of wavelength [27]. Because of the extreme breadth of the spectrum, light generated in the spectral wings is not resonant in the laser cavity and thus is not forced to obey the cavity transverse spatial mode conditions. This results in the production of non-Gaussian modes (figure 6), which cause poor mode matching between the ν and 2ν portions of the spectrum. The change in spot size of the beam as a function of wavelength, observed in figure 6, is the result of a sudden decrease in waist size for light in the wings of the spectrum.

Being able to combine the characteristics of two or more mode-locked lasers working at different wavelengths certainly provides an ultimately flexible approach to coherent control. The capability of synchronizing the repetition rates and phase locking the carrier frequencies of multiple mode-locked lasers opens many applications. Working with two independent femtosecond lasers operating in different wavelength regions, we have synchronized the relative timing between the two pulse trains at the femtosecond level [28, 29] and also phase locked the two carrier frequencies [30], thus establishing phase coherence between the two lasers. By coherently stitching optical bandwidths together, a 'synthesized' pulse has been generated [31]. With the same pair of Ti : sapphire mode-locked lasers, we have

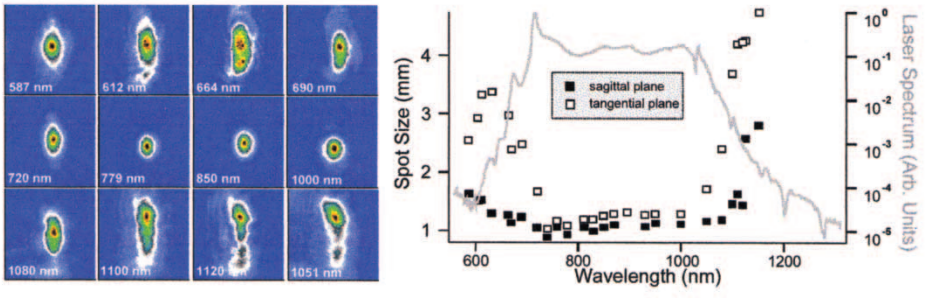

Figure 6. The laser beam profile for selected wavelengths. A 10–90 knife-edge fit was used to determine the spot sizes in the sagittal (■) and tangential (□) planes, displayed on the right of the figure. (Some of the diffraction rings observed for the larger beam modes may result from aperturing of the laser mirrors.)

demonstrated widely tuneable femtosecond pulse generation in the mid- and far-infrared using difference-frequency generation [32]. The flexibility of this new experimental approach is evidenced by the capability of rapid and programmable switching and modulation of the wavelength and amplitude of the generated infrared pulses. A fully developed capability of producing phase-coherent visible and infrared pulses over a broad spectral bandwidth, coupled with the capability of an optical waveform synthesizer with arbitrary control in amplitude and pulse shape, represents the ultimate instrumentation for coherent control of molecular systems [33]. For frequency metrology and precision molecular spectroscopy in the infrared region, we note that the difference-frequency generation approach produces an absolute-frequency-calibrated infrared comb when the two Ti : sapphire lasers are synchronized and share a common offset frequency f_0.

To establish phase coherence among independent ultrafast lasers, it is necessary to first achieve a level of synchronization among the lasers so that the remaining timing jitter is less than the oscillation period of the optical carrier, namely 2.7 fs for lasers centred around 800 nm. In the push for greater stability and precision of femtosecond optical combs, a number of effective techniques for ultralow-jitter synchronization have emerged. They include an all-electronic approach for active stabilization of repetition rates [28, 29, 34], cross-phase modulation to synchronize passively two mode-locked lasers that share the same intracavity gain medium [35], linking repetition rates of lasers to the same optical standard [36], and optical cross-correlation between the pulse trains to be synchronized [37].

Detecting timing jitter should be carried out at a high harmonic of f_{rep} to attain much enhanced detection sensitivity. The harmonic order can range from 10 to 10^6. This approach has enabled tight synchronization between two independent mode-locked Ti : sapphire lasers with a residual rms-timing jitter of the order of 1 fs or less, integrated over a bandwidth of a few megahertz. Of course, enhanced detection sensitivity comes with the price of reduced dynamic range for the change in the nominal value of f_{rep}. This problem can be alleviated by invoking another control loop that works with lower harmonics of f_{rep}. The low-frequency control loop can be used to achieve a desired timing offset between the two pulse trains. The high-stability loop can then be activated to achieve the ultimate level of synchronization at the preset value of timing offset. For example, in the all-electronic implementation of laser synchronization, we use two phase-locked loops. One phase-locked loop compares and locks the fundamental repetition frequencies (100 MHz) of the lasers. The second high-resolution phase-locked loop compares the phase of the 140th harmonic of the two repetition frequencies at 14 GHz. A transition of control from the first to the second phase-locked loop is implemented smoothly to allow synchronization at the femtosecond level to be maintained for any timing offsets within the entire dynamic range, for example one pulse period of 10 ns [29]. The synchronization lock can be maintained for several hours.

The present level of pulse synchronization would make it possible to take full advantage of this femtosecond time resolution for applications such as high power sum- and difference-frequency mixing [32, 38], novel pulse generation and shaping [31], new generations of laser- and accelerator-based light sources, or experiments requiring synchronized laser light and X-rays or electron beams from synchrotrons [39]. Indeed, accurate timing of high-intensity fields is essential for

several important schemes in quantum coherent control and extreme nonlinear optics such as efficient X-ray generation.

Phase locking of separate femtosecond lasers requires a step beyond tight synchronization of the two pulse trains. One needs effective detection and stabilization of the phase difference between the two optical carrier waves underlying the pulse envelopes [30, 40]. After synchronization matches the repetition rates ($f_{\mathrm{rep}\ 1} = f_{\mathrm{rep}\ 2}$), phase locking requires that the spectral combs of the individual lasers are maintained exactly coincident in the region of spectral overlap so that the two sets of optical frequency combs form a continuous and phase-coherent entity. We detect a coherent heterodyne-beat signal between the corresponding comb components of the two lasers. Such heterodyne detection yields information related to the difference in the offset frequencies of the two lasers, $\Delta f_0 = f_{0\ 1} - f_{0\ 2}$, which can then be controlled. By phase locking Δf_0 to a frequency of a mean-zero value, we effectively demand that $\Delta\phi_{\mathrm{CE1}} - \Delta\phi_{\mathrm{CE2}} = 0$, leading to two pulse trains that have nearly identical phase evolutions. When stabilized, fluctuations associated with the recorded beat-frequency signal Δf_0 can be suppressed to just a few millihertz with an averaging time of 1 s. This is shown in figure 7. Such a capability has already been used to transfer optical clock signals from a Ti : sapphire mode-locked laser to mode-locked laser sources operating at 1.5 μm for precise and accurate transfer of timing signals over a long-distance optical fibre network [40, 41].

The established phase coherence between the two femtosecond lasers can also be revealed via a direct time-domain analysis. For example, as shown in figure 8, spectral interferometry analysis of the joint spectra of the two pulses produces interference fringes that correspond to phase coherence between the two pulse trains persisting over the measurement time period. A cross-correlation measurement between the two pulse trains also manifests phase coherence in the display of persistent fringe patterns. A more powerful and straightforward demonstration of the 'coherently synthesized' aspect of the combined pulse is through a second-order autocorrelation measurement of the combined pulse. For this measurement, the two pulse trains are maximally overlapped in the time domain before the

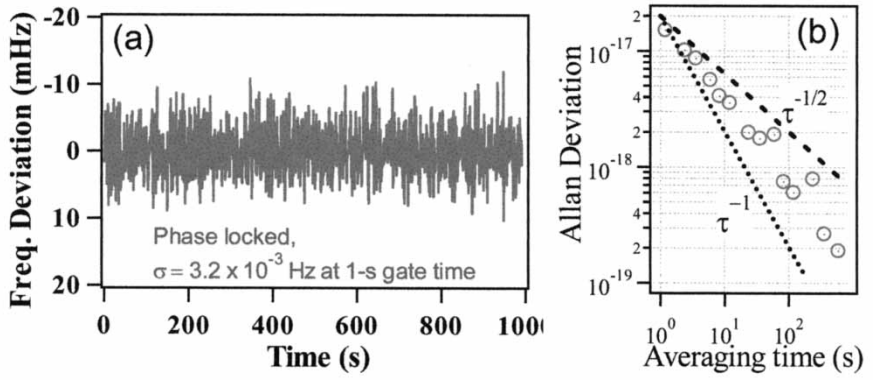

Figure 7. (a) Heterodyne beat between the carrier frequencies of two phase-stabilized femtosecond lasers. The beat frequency is recorded by a frequency counter at 1 s gate time. (b) Allan deviation is determined from the frequency-counting record, showing the long-term instability of the beat frequency.

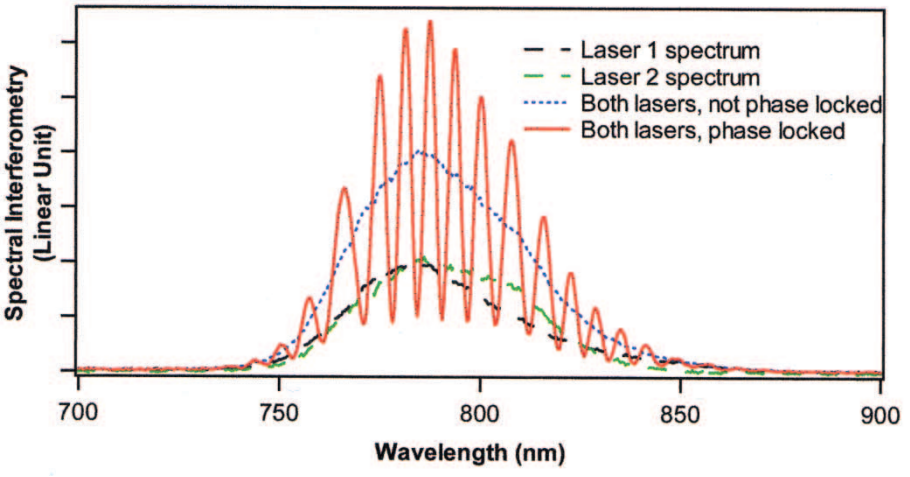

Figure 8. Spectral interferometry measurement of the established coherence between the two phase-locked femtosecond lasers: (——), two curves representing the spectra of the individual laser's; (- - -), combined spectrum of the two lasers when they are not phase locked; (—), clear interference fringes between the two laser spectra when they are phase locked.

autocorrelator. When the two femtosecond lasers are phase locked, autocorrelation reveals a clean pulse that is often shorter in apparent duration and larger in amplitude than the original individual pulses. A successful implementation of coherent light synthesis has therefore become reality; the coherent combination of output from more than one laser where the combined output can be viewed as a coherent femtosecond pulse being emitted from a single source [31].

The capability to control pulse timing and the pulse-carrier phase precisely allows one to manipulate pulses using novel techniques and achieve unprecedented levels of flexibility and precision. Here we point out another powerful experimental approach that utilizes this capability. Simultaneous control of timing jitter and carrier-envelope phase has now been used to superpose phase coherently a collection of successive pulses from a mode-locked laser. By stabilizing the two degrees of freedom of a pulse train incident to an optical cavity acting as a coherent delay, constructive interference of sequential pulses will be built up. The coherently enhanced pulse stored in the cavity can be switched out using a cavity-dumping element (such as a Bragg cell), resulting in a single phase-coherent amplified pulse [42]. Such a scheme is illustrated in figure 9, showing the matching of the pulse repetition period with the cavity round trip time. The build-up factor is determined ideally by the cavity finesse and the cavity input-coupling coefficient, when appropriate intracavity dispersion compensation has been implemented.

The use of a passive cavity also offers the unique ability to amplify pulses effectively in spectral regions where no suitable gain medium exists such as for the infrared pulses from difference-frequency mixing or the ultraviolet light from harmonic generation. Unlike actively dumped laser systems, the pulse energy is not limited by the saturation of a gain medium or the requirement for a saturable absorber for mode locking. Instead, the linear response of the passive cavity allows

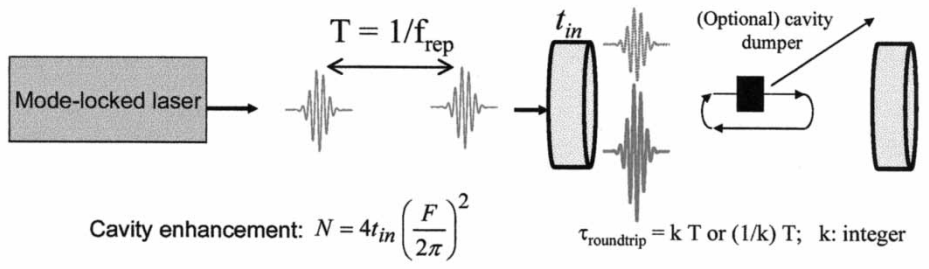

Figure 9. Principle of the coherent pulse amplification scheme with the aid of an optical cavity, showing the matching of the pulse repetition period with the cavity round-trip time. The intracavity pulse is switched out when sufficient energy is built up in the cavity. The build-up factor is given ideally by the cavity finesse, with appropriate intracavity dispersion compensation.

the pulse energy to build up inside the cavity until limited by cavity loss and/or dispersive pulse spreading. Therefore storage and amplification of ultrashort pulses in the femtosecond regime require precise control of the reflected spectral phase of the resonator mirrors and the optical loss of the resonator. While the reflected group delay of the mirrors only changes the effective length of the resonator, the group delay dispersion (GDD) and higher-order derivatives of the group delay with respect to frequency affect the pulse shape. The net cavity GDD over the bandwidth of the pulse needs to be minimized to maintain the shape of the resonant pulse and to allow for the coherent addition of energy from subsequent pulses.

The combination of ultrashort pulse trains and optical cavities will provide opportunities for a variety of exciting experiments. An immediate impact is on precision stabilization of ultrafast lasers [43, 44]. Similar to the state-of-art stabilization of CW lasers, a cavity-stabilized ultrafast laser is expected to demonstrate superior short-term stability of both the pulse repetition frequency and the carrier-envelope phase. The improved stability is beneficial in particular for time-domain applications where the signal-processing bandwidth is necessarily large. Another attractive application lies in broadband and ultrasensitive spectroscopy. The use of high-finesse cavities has played a decisive role for enhancing sensitivity and precision in atomic and molecular spectroscopy. We expect a dramatic advancement in the efficiency of intracavity spectroscopy by exploiting the application of ultrashort pulses. In other words, high detection sensitivity is achievable uniformly across the broad spectrum of the pulse. Applying cavity stabilization techniques to femtosecond lasers, the comb structure of the probe laser can be precisely matched to the resonance modes of an empty cavity, allowing an efficient energy coupling for a spectroscopic probe. Molecular samples located inside the high-finesse cavity will alter the cavity-transmitted pulse spectrum in a sensitive manner. Preliminary data on spectrally resolved time-domain ring-down measurement for intracavity loss over the entire femtosecond laser bandwidth are already quite promising. To develop sources for ultrafast nonlinear spectroscopy, a properly designed dispersion-compensated cavity housing a nonlinear crystal will provide efficient nonlinear optical frequency conversion of ultrashort optical pulses in spectral regions where no active gain medium exists. Furthermore, by simultaneously locking two independent mode-locked lasers to the same optical cavity,

efficient-sum and/or difference-frequency generation can be produced over a large range of wavelengths. Extreme nonlinear optics experiments may be carried out inside the passive optical cavity where samples of interest are located to interact with a high-repetition-rate pulse train with much enhanced peak powers.

We have applied the coherent pulse-stacking technique to both picosecond and femtosecond pulses. Initial studies have already demonstrated amplification of picosecond pulses of greater than 30 times at repetition rates of 253 kHz, yielding pulse energies greater than 150 nJ [45]. With significant room left for optimization of the cavity finesse (current value of about 350, limited by the cavity input-coupling mirror), we expect that amplifications greater than one hundred times are feasible, which would bring pulse energies into the microjoule range. Such a passive picosecond-pulse 'amplifier', together with the synchronization technique that we developed for pulse synthesis, has made a strong impact on the field of nonlinear-optics-based spectroscopy and imaging of biomolecular systems, showing significant improvements in experimental sensitivity and spatial resolution [46, 47]. With the enhanced detection sensitivity comes the capability of tracking real-time biological dynamics.

While the use of picosecond pulses allows us to separate out complications arising from intracavity dispersion, for sub-100 fs pulses, dispersive phase shifts in the cavity mirrors become an important topic. Preliminary results in enhancing low-individual-pulse energies for sub-50 fs pulses illustrate the importance of GDD control. The external enhancement cavity incorporated specially designed negative-GDD low-loss mirrors to compensate simultaneously for 3 mm of fused silica in the Bragg cell and to provide high finesse. The input-coupling mirror transmission was about 0.8% with a measured cavity finesse of 440. An intracavity energy build-up ratio of about 130 is expected, leading to single-pulse amplifications of approximately 52 for the current set-up, given the 40% dumping efficiency of our Bragg cell. The negative-GDD mirrors were designed to compensate only partially for the total cavity dispersion. The remaining cavity GDD was estimated at between +20 and +30 fs^2. Controlling the intracavity pressure allows fine tuning of the net cavity GDD to zero. Experimental results are in good agreement with independent numerical calculations. The input pulses of 47 fs duration are experimentally enhanced by a factor of about 120 inside the passive cavity, with the output pulses broadened only to about 49 fs. These results are shown in figure 10. Our recent experimental results have extended this femtosecond pulse amplification by a passive optical cavity into the sub-40 fs regime, with a net out-of-cavity amplification factor of the order of 50 [48].

Control of molecular reactions is a central goal of chemistry. The development of the laser led to the proposal that light fields could be used to control reaction pathways (for recent reviews, see [33] and [49]). Many techniques are sensitive to the phase of the applied fields and thus dubbed 'coherent control'. To date, only the relative phase between two laser fields, or the relative internal phase of a femtosecond pulse (i.e. its chirp), has been demonstrated to have physical impacts. Some new schemes explore interference between pathways involving n-photons and m-photons. When n and m have opposite parity, a dependence on ϕ_{CE} will occur for excitation by a single ultrashort pulse. Early studies demonstrated the interference phenomenon by using a pair of pulses, which had their relative phases controlled, to ionize rubidium [50] and to control electrical currents in bulk semiconductors [51, 52]. In both cases, there is a connection between spatial

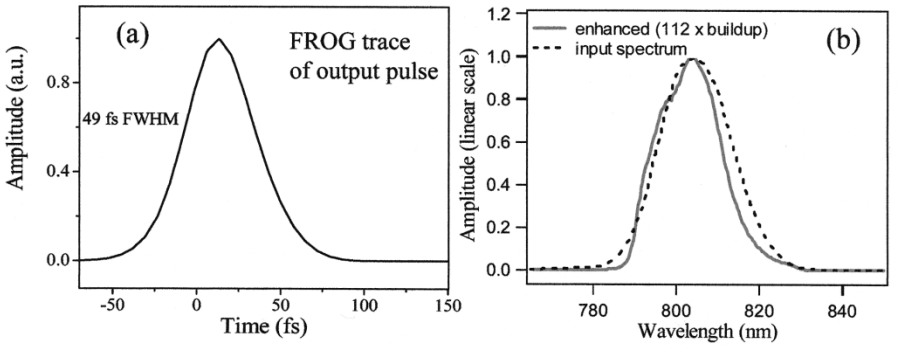

Figure 10. Coherent evolution of a 50 fs pulse inside the cavity. (a) Frequency-resolved optical-gating measurement of the amplified pulse switched out of the passive cavity shown a full width at half-maximum (FWHM) of 49 fs, slightly wider than the input pulse width of 47 fs. (b) Comparison of the input and output pulse spectra, showing no significant distortion to the input pulse spectrum after the intracavity power is built up by a factor of 112.

direction and the relative phase. The latter system has recently been shown to be sensitive to ϕ_{CE} [52].

In a semiconductor, the phase sensitivity can be understood by considering the **k** dependence of the transition amplitudes. In GaAs, when the phase is such as to produce constructive interference between one- and two-photon absorption at $-\mathbf{k}$, it produces, to a good approximation, destructive interference at **k**. This effect is schematically shown in figure 11. For an octave-spanning pulse, the frequency components for one-photon absorption come from the high-energy tail of the spectrum, while for the two-photon absorption they come from the low-frequency tail. Thus ϕ_{CE} determines their relative phase in a manner analogous to the beat signal that occurs in a standard ν-to-2ν interferometer. The non-interfering carrier populations do not contribute to the signal, which makes it intrinsically balanced and thus insensitive to amplitude fluctuations [53]. This insensitivity provides an advantage over the standard ν-to-2ν interferometer, which relies on an ordinary photodiode for conversion of the light to an electrical signal.

The experimental demonstration of quantum interference control of the injected photocurrent in a semiconductor is shown in figure 12 [52]. The carrier-envelope evolution of the laser is stabilized so that $f_0 = 2400$ Hz using a standard ϕ_{CE} interferometer in a servo loop. A portion of the resulting phase-stabilized pulse train is then used to illuminate a low-temperature-grown GaAs sample with gold electrodes. The electrodes are used to collect the resulting photocurrent, which also oscillates at f_0.

We use lock-in detection to demonstrate the sensitivity of quantum interference in a semiconductor to small static shifts in the carrier-envelope phase, which show up as a change in ϕ_0. Lock-in detection of a stable amplitude signal, owing to the narrow detection bandwidth, is strongly affected by the coherence of the laser offset frequency. As a result, for lock-in detection of injected photocurrents, coherence in the carrier-envelope phase is a prerequisite.

To change ϕ_0, we insert a 176 μm zinc borosilicate plate after the microstructure fibre and before the interferometer used to lock the laser offset frequency. The

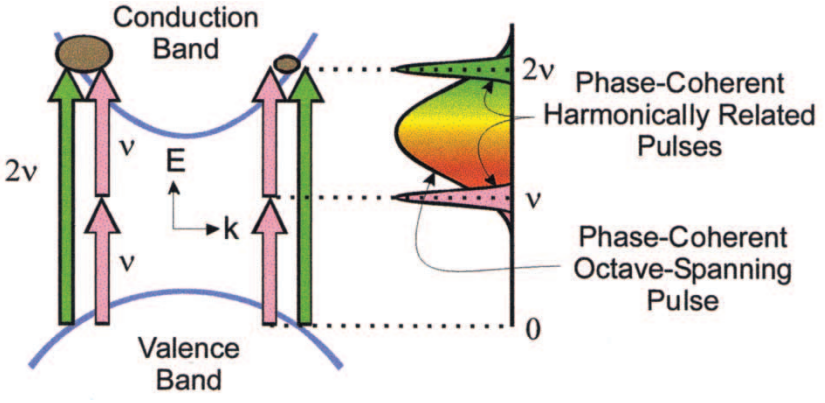

Figure 11. Conceptual diagram of quantum interference between one- and two-photon absorption in a direct-gap semiconductor. The two interfering absorption pathways are driven by the spectral wings of a single octave-spanning pulse. An imbalance in the otherwise symmetric carrier population distribution in momentum space (represented by ovals), occurs owing to interference and results in a net current. The resulting photocurrent is sensitive to ϕ_{CE}.

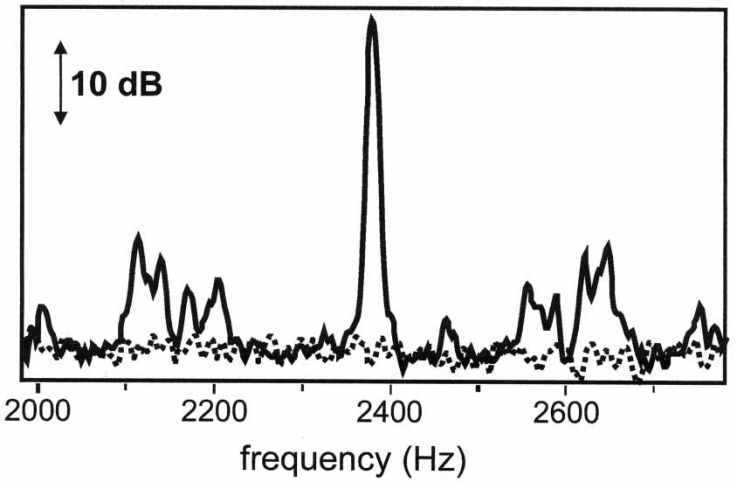

Figure 12. Spectrum of the measured quantum interference signal in a semiconductor: (▪▪▪▪), background (no light on the sample).

small phase difference due to dispersion of the glass plate facilitates fine tuning of ϕ_0. Rotation of the glass plate results in shifts in ϕ_{CE}, which are measured by the ν-to-2ν interferometer. The stabilization loop compensates for the ensuing phase error by adjusting ϕ_0 of the laser output, which is then measured as an offset in the phase of the interference signal (figure 13 (a)). The measured phase shifts in figure 13 (a) versus plate rotation are compared with those calculated using the dispersion and thickness of the glass plate (see figure 13 (b)). The measured and calculated changes correspond well up to a plate rotation angle of 30°, where the observed discrepancy may be the result of beam misalignment into the ν-to-2ν interferometer.

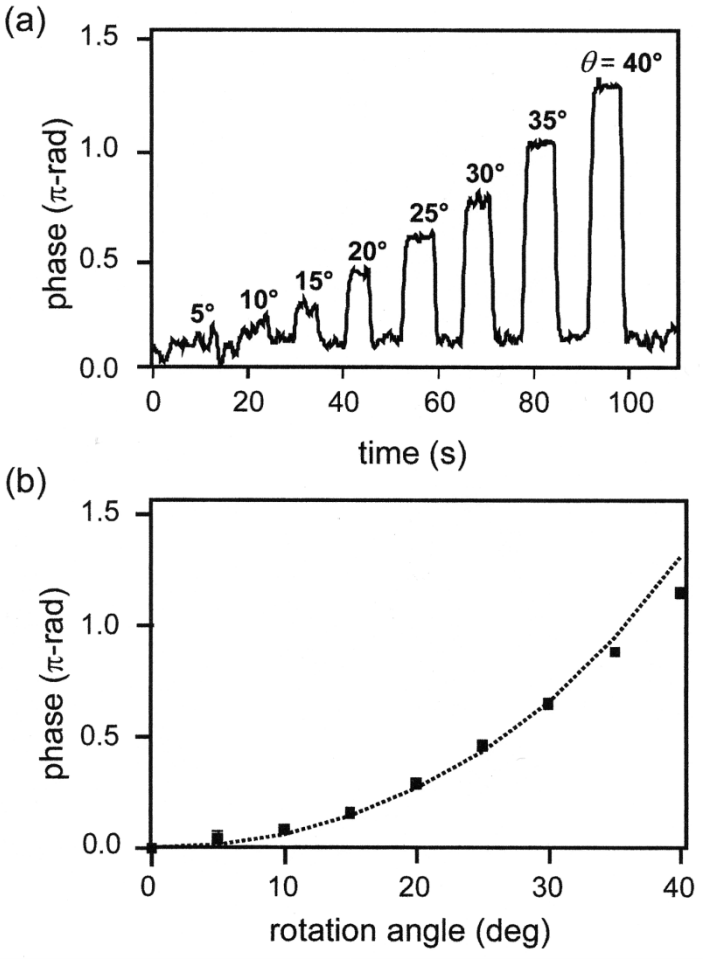

Figure 13. (a) Phase of the quantum interference control signal as measured relative to the reference used for laser stabilization. The time record of the quantum interference control phase (100 ms time constant) shows the phase jumps associated with rotations of the glass plate from 0° to θ and back again for eight different rotation angles. (b) Comparison between the phase change measured in (a) (■) and the calculated carrier-envelope phase change (- - -).

These results provide an interesting route to a simple solid-state detector of the carrier-envelope phase. Recent measurements show that the measurement of $S(\nu)$ using quantum interference gives comparable results with using a standard ν-to-2ν interferometer and that there is no conversion of amplitude fluctuations to phase [53]. The first step is to use it simply to stabilize f_0. However, this requires a significant improvement in signal-to-noise ratio and bandwidth. This technique does not suffer from the arbitrary offsets that plague detection using a standard ν-to-2ν interferometer and thus may allow measurement of the 'absolute' ϕ_{CE} [54]. Shifts due to dispersion in the GaAs detector still need to be considered.

The ability to stabilize the carrier-envelope phase evolution of mode-locked lasers has also had tremendous impact on the fields of optical frequency metrology

and optical atomic clocks. Both fields require that a phase-coherent connection be established between rf frequencies and optical frequencies. Previously this connection was made using complex frequency chains [55, 56]. However, it is now possible to do this with a single mode-locked laser because controlling $\Delta\phi_{CE}$ means that the optical frequencies of the comb are completely defined in terms of the two rf frequencies f_0 and f_{rep}. This relationship enables the measurement of optical frequencies relative to caesium clocks [14, 19, 57]. The process can also be reversed locking the comb to an optical transition allows it to serve as a clockwork to establish a microwave output; that is, it is an optical atomic clock [21, 58, 59]. For a recent review of these fields, see reference [60].

The ability to control the carrier-envelope phase evolution in mode-locked lasers has resulted from a remarkable synergy between ultrafast techniques and those developed for precision laser stabilization. It is having a significant impact on a number of fields, not the least of which is the generation attosecond pulses and measurement of processes on attosecond time scales.

Acknowledgments

Many at JILA have contributed to this work; the authors would particularly like to acknowledge the contributions of T.M. Fortier, S.M. Foreman, K.W. Holman, D.J Jones, R.J. Jones, L.-S. Ma, P.A. Roos, R. Shelton, J.L. Hall and S.A. Diddams. This work is supported by the National Institute of Standards and Technology, the National Science Foundation, the Office of Natural Research and the Air Force Office of Scientific Research.

References

[1] Diels, J.-C., and Rudolph, W., 1996, *Ultrashort Laser Pulse Phenomena: Fundamentals, Techniques, and Applications on a Femtosecond Timescale* (San Diego, California: Academic Press).
[2] Ippen, E. P., 1994, *Appl. Phys.* B, **58,** 159.
[3] Fork, R. L., Martinez, O. E., and Gordon, J. P., 1984, *Optics Lett.*, **9,** 150.
[4] Spence, D. E., Kean, P. N., and Sibbett, W., 1991, *Optics Lett.*, **16,** 42.
[5] Negus, D. K., Spinelli, L., Goldblatt, N., and Feugnet, G., 1991, *Advanced Solid-State Lasers* (Washington, DC: Optical Society of America).
[6] Asaki, M. T., Huang, C. P., Garvey, D., Zhou, J. P., Kapteyn, H. C., and Murnane, M. M., 1993, *Optics Lett.*, **18,** 977.
[7] Morgner, U., Kärtner, F. X., Cho, S. H., Chen, Y., Haus, H. A., Fujimoto, J. G., Ippen, E. P., Scheuer, V., Angelow, G., and Tschudi, T., 1999, *Optics Lett.*, **24,** 411.
[8] Sutter, D. H., Steinmeyer, G., Gallmann, L., Matuschek, N., Morier-Genoud, F., Keller, U., Scheuer, V., Angelow, G., and Tschudi, T., 1999, *Optics Lett.*, **24,** 631.
[9] Ell, R., Morgner, U., Kärtner, F. X., Fujimoto, J. G., Ippen, E. P., Scheuer, V., Angelow, G., Tschudi, T., Lederer, M. J., Boiko, A., and Luther-Davies, B., 2001, *Optics Lett.*, **26,** 373.
[10] Fortier, T. M., Jones, D. J., and Cundiff, S. T., 2003, *Optics Lett.*, **28,** 2198.
[11] Reichert, J., Holzwarth, R., Udem, T., and Hänsch, T. W., 1999, *Optics Commun.*, **172,** 59.
[12] Cundiff, S. T., 2002, *J. Phys.* D, **35,** R43.
[13] Xu, L., Spielmann, C., Poppe, A., Brabec, T., Krausz, F., and Hänsch, T. W., 1996, *Optics Lett.*, **21,** 2008.

[14] Jones, D. J., Diddams, S. A., Ranka, J. K., Stentz, A., Windeler, R. S., Hall, J. L., and Cundiff, S. T., 2000, *Science*, **288,** 635.
[15] Telle, H. R., Steinmeyer, G., Dunlop, A. E., Stenger, J., Sutter, D. H., and Keller, U., 1999, *Appl. Phys.* B, **69,** 327.
[16] Apolonski, A., Poppe, A., Tempea, G., Spielmann, C., Udem, T., Holzwarth, R., Hänsch, T. W., and Krausz, F., 2000, *Phys. Rev. Lett.*, **85,** 740.
[17] Ranka, J. K., Windeler, R. S., and Stentz, A. J., 2000, *Optics Lett.*, **25,** 25.
[18] Ranka, J. K., Windeler, R. S., and Stentz, A. J., 2000, *Optics Lett.*, **25,** 796.
[19] Diddams, S. A., Jones, D. J., Ye, J., Cundiff, T., Hall, J. L., Ranka, J. K., Windeler, R. S., Holzwarth, R., Udem, T., and Hänsch, T. W., 2000, *Phys. Rev. Lett.*, **84,** 5102.
[20] Ye, J., Hall, J. L., and Diddams, S. A., 2000, *Optics Lett.*, **25,** 1675.
[21] Ye, J., Ma, L. S., and Hall, J. L., 2001, *Phys. Rev. Lett.*, **87,** 270 801.
[22] Dietrich, P., Krausz, F., and Corkum, P. B., 2000, *Optics Lett.*, **25,** 16.
[23] Paulus, G. G., Grasbon, F., Walther, H., Villoresi, P., Nisoli, M., Stagira, S., Priori, E., and De Silvestri, S., 2001, *Nature*, **414,** 182.
[24] Ye, J., Cundiff, S. T., Foreman, S., Fortier, T. M., Hall, J. L., Holman, K. W., Jones, D. J., Jost, J. D., Kapteyn, H. C., Leeuwen, K., Ma, L. S., Murnane, M. M., Peng, J. L., and Shelton, R. K., 2002, *Appl. Phys.* B, **74,** S27.
[25] Fortier, T. M., Jones, D. J., Ye, J., Cundiff, S. T., and Windeler, R. S., 2002, *Optics Lett.*, **27,** 1436.
[26] Matos, L., Kleppner, D., Kuzucu, O., Schibli, T. R., Kim, J., Ippen, E. P., and Kaertner, F. X., 2004, *Optics Lett.*, **29,** 1683.
[27] Cundiff, S. T., Knox, W. H., Ippen, E. P., and Haus, H. A., 1996, *Optics Lett.*, **21,** 662.
[28] Ma, L.-S., Shelton, R. K., Kapteyn, H. C., Murnane, M. M., and Ye, J., 2001, *Phys. Rev.* A, **64,** 021 802.
[29] Shelton, R. K., Foreman, S. M., Ma, L. S., Hall, J. L., Kapteyn, H. C., Murnane, M. M., Notcutt, M., and Ye, J., 2002, *Optics Lett.*, **27,** 312.
[30] Shelton, R. K., Ma, L. S., Kapteyn, H. C., Murnane, M. M., Hall, J. L., and Ye, J., 2002, *J. Mod. Optics*, **49,** 401.
[31] Shelton, R. K., Ma, L. S., Kapteyn, H. C., Murnane, M. M., Hall, J. L., and Ye, J., 2001, *Science*, **293,** 1286.
[32] Foreman, S. M., Jones, D. J., and Ye, J., 2003, *Optics Lett.*, **28,** 370.
[33] Rabitz, H., de Vivie-Riedle, R., Motzkus, M., and Kompa, K., 2000, *Science*, **288,** 824.
[34] Jones, D. J., Holman, K. W., Notcutt, M., Ye, J., Chandalia, J., Jiang, L. A., Ippen, E. P., and Yokoyama, H., 2003, *Optics Lett.*, **28,** 813.
[35] Leitenstorfer, A., Furst, C., and Laubereau, A., 1995, *Optics Lett.*, **20,** 916.
[36] Bartels, A., Diddams, S. A., Ramond, T. M., and Hollberg, L., 2003, *Optics Lett.*, **28,** 663.
[37] Schibli, T. R., Kim, J., Kuzucu, O., Gopinath, J. T., Tandon, S. N., Petrich, G. S., Kolodziejski, L. A., Fujimoto, J. G., Ippen, E. P., and Kaertner, F. X., 2003, *Optics Lett.*, **28,** 947.
[38] Kaindl, R. A., Wurm, M., Reimann, K., Hamm, P., Weiner, A. M., and Woerner, M., 2000, *J. Opt. Soc. Am.* B, **17,** 2086.
[39] Schoenlein, R. W., Leemans, W. P., Chin, A. H., Volfbeyn, P., Glover, T. E., Balling, P., Zolotorev, M., Kim, K. J., Chattopadhyay, S., and Shank, C. V., 1996, *Science*, **274,** 236.
[40] Holman, K. W., Jones, D. J., Ye, J., and Ippen, E. P., 2003, *Optics Lett.*, **28,** 2405.
[41] Holman, K. W., Jones, D. J., Hudson, D. D., and Ye, J., 2004, *Optics Lett.*, **29,** 1554.
[42] Jones, R. J., and Ye, J., 2002, *Optics Lett.*, **27,** 1848.
[43] Jones, R. J., and Diels, J. C., 2001, *Phys. Rev. Lett.*, **86,** 3288.
[44] Jones, R. J., Thomann, I., and Ye, J., 2004, *Phys. Rev.* A, **69,** 051803 (R).
[45] Potma, E. O., Evans, C., Xie, X. S., Jones, R. J., and Ye, J., 2003, *Optics Lett.*, **28,** 1835.
[46] Potma, E. O., Jones, D. J., Cheng, J. X., Xie, X. S., and Ye, J., 2002, *Optics Lett.*, **27,** 1168.

[47] Jones, D. J., Potma, E. O., Cheng, J. X., Burfeindt, B., Pang, Y., Ye, J., and Xie, X. S., 2002, *Rev. Scient. Instrum.*, **73,** 2843.
[48] Jones, R. J., and Ye, J., 2004, *Optics Lett.* (in press).
[49] Shapiro, M., and Brumer, P., 2000, *Adv. ato. Molec. opt. Phys.*, **42,** 287.
[50] Yin, Y.-Y., Chen, C., Elliot, D. S., and Smith, A. V., 1992, *Phys. Rev. Lett.*, **69,** 2353.
[51] Haché, A., Sipe, J. E., and van Driel, H. M., 1998, *IEEE J. Quant. Electron.*, **34,** 1144.
[52] Fortier, T. M., Roos, P. A., Jones, D. J., Cundiff, S. T., Bhat, R. D. R., and Sipe, J. E., 2004, *Phys. Rev. Lett.*, **92,** 147 403.
[53] Roos, P. A., Li, X., Pipis, J., and Cundiff, S. T., 2004, *Opt. Expr.*, **12**, 4255.
[54] Jones, D. J., Fortier, T. M., and Cundiff, S. T., 2004, *J. Opt. Soc. Am.* B, **21,** 1098.
[55] Evenson, K. M., Wells, J. S., Mullen, L. O., and Day, G. W., 1972, *Appl. Phys. Lett.*, **20,** 133.
[56] Schnatz, H., Lipphardt, B., Helmcke, J., Riehle, F., and Zinner, G., 1996, *Phys. Rev. Lett.*, **76,** 18.
[57] Holzwarth, R., Udem, T., Hänsch, T. W., Knight, J. C., Wadsworth, W. J., and Russell, P. S. J., 2000, *Phys. Rev. Lett.*, **85,** 2264.
[58] Diddams, S. A., Udem, T., Bergquist, J. C., Curtis, E. A., Drullinger, R. E., Hollberg, L., Itano, W. M., Lee, W. D., Oates, C. W., Vogel, K. R., and Wineland, D. J., 2001, *Science*, **293,** 825.
[59] Wilpers, G., Binnewies, T., Degenhardt, C., Sterr, U., Helmcke, J., and Riehle, F., 2002, *Phys. Rev. Lett.*, **89,** 230 801.
[60] Cundiff, S. T., and Ye, J., 2003, *Rev. Mod. Phys.*, **75,** 325.